Desulfurization of SO₂ and Thiophene on Surfaces and Nanoparticles of Molybdenum Carbide: Unexpected Ligand and Steric Effects

Ping Liu, José A. Rodriguez,* and James T. Muckerman

Department of Chemistry, Brookhaven National Laboratory, Bldg. 555, Upton, New York 11973

Received: March 31, 2004; In Final Form: July 20, 2004

The destruction of S-containing molecules is a very important issue in the chemical industry and the control of environmental pollution. The desulfurization of sulfur dioxide and thiophene on molybdenum carbide surfaces, α-Mo₂C(001) and δ-MoC(001), and on a Mo₈C₁₂ nanoparticle was studied with density functional theory. Our study reveals unexpected ligand and steric effects. The Mo₈C₁₂ nanoparticle behaves as actively as α-Mo₂C(001) toward SO₂ despite the high C/Mo ratio and C₂ groups. In contrast, SO₂ bonds weakly with δ-MoC(001). Spontaneous S−O bond cleavage was observed on both Mo₈C₁₂ and α-Mo₂C(001). Contrary to common assumptions, the C atoms are not simple spectators and play a key role in the energetics for the dissociation of SO₂. In the case of thiophene adsorption, only α-Mo₂C(001) exhibits a high chemical activity that leads to a spontaneous S−C bond cleavage. The interaction of thiophene with both δ-MoC(001) and Mo₈C₁₂ is weak. On the nanoparticle, steric repulsion between the C₂ groups and thiophene overcomes the high reactivity of the Mo atoms in corner or edge sites. Our results illustrate the interplay of ligand and steric effects in nanoparticles of metal compounds.

I. Introduction

Sulfur-containing molecules, especially sulfur dioxide (SO₂) and thiophene (C₄H₄S), have received a lot of attention for decades due to their negative impact in our industrial society.[1] SO₂ is a serious air pollutant (frequently produced during the combustion of fossil derived fuels) that contributes to the generation of acid rain, and is also known as a corrosive gas and catalyst poison.[1] C₄H₄S and its derivatives are common impurities in petroleum, and they must be removed in oil refineries through the important process of hydrodesulfurization (HDS).[1] It has been indicated that C₄H₄S is particularly difficult to desulfurize in this process.[2] Therefore, an extensive effort has been focused on the search for chemical compounds with a high efficiency for breaking the S−O bonds in SO₂ and the C−S bonds in C₄H₄S.[3−23] Recent legislation also emphasizes the need for reducing the sulfur content in oil-derived fuels and for controlling the emissions of SO₂ in industrial operations.

Molybdenum compounds can be useful in desulfurization processes.[2,17,21a−c,23,24−27] The industrial catalysts for HDS typically involve MoS₂ supported on alumina with Ni or Co as promoters.[26,27] These are complex systems that can contain more than one phase,[2,26,27] and recent studies indicate that molybdenum sulfide under reaction conditions is partially transformed into a carbide (MoCₓS₂−ₓ) where the HDS reactions occur.[27b] Molybdenum carbide and nitride catalysts have shown the potential to replace sulfided Mo catalysts in HDS reactions.[11,12,24,28] It has been found that the carbide generally has higher HDS rates than the nitride, which are twice greater than those of commercial catalysts.[28] However, despite of the fact that Mo carbides have a high activity as HDS catalysts, not much is known about the fundamental interactions of S-containing molecules with these compounds. Previous studies have used X-ray photoelectron spectroscopy, temperature-programmed desorption, and X-ray absorption near-edge spectroscopy to examine the chemistry of SO₂, H₂S, and C₄H₄S on surfaces of Mo₂C or carbide-modified Mo(110).[17,23,24,29] These systems exhibit a very high reactivity and the cleavage of the S−O, H−S, and C−S bonds occurs at temperatures below 250 K. It is not clear how the desulfurization activity will change when the C/Mo ratio increases in a molybdenum carbide. It is commonly assumed that the C centers in a carbide are simple spectators in HDS reactions.[23,24,27b] Thus, an increase in the C/Mo ratio should lead to deactivation as a consequence of two factors.[17,23,24] One is a ligand effect; the other is an ensemble effect. By increasing the C concentration, Mo atoms in the carbide will become more inert due to an electronic structure modified by C (a substantial electron transfer from Mo to C[30−32] and a d-band center shifted downward, ligand effect), and the number of active Mo sites that can be exposed on the surface will decrease (ensemble effect[24]). The direct participation of the C sites in the desulfurization process could lead to a much more complex situation.[5] Another important issue is how the desulfurization activity of a carbide varies when going from nanoparticles to bulk surfaces. In practical applications small particles of molybdenum carbide are dispersed on catalyst supports,[24] and size effects could induce special chemical properties not seen for the bulk compounds.[24a,33,34]

With recent improvements density functional theory (DFT) is capable of providing qualitative and, in many cases, quantitative insights into surface science and catalysis.[5,33,35] In the present paper, we carry out a set of DFT calculations to systematically study the adsorption properties of SO₂ and C₄H₄S on Mo carbides, including bulk surfaces such as α-Mo₂C(001) and δ-MoC(001) as well as the metallocarbohedrene (metcar) Mo₈C₁₂ nanoparticle. Metcars have become a highlight of metal−carbide studies recently.[30,31,33,36,37] Interest in these carbide molecules stems from their unusual properties including ionization, bonding, and reactivity.[33,36,37] In principle, α-Mo₂C-(001), δ-MoC(001), and Mo₈C₁₂ have different structures and

* Address correspondence to this author, E-mail: rodrigez@bnl.gov. Fax: 631-344-5815.

Desulfurization of SO₂ and Thiophene

J. Phys. Chem. B, Vol. 108, No. 40, 2004 **15663**

different C concentrations on the surface. This makes them perfect candidates for examining possible correlations between the C/Mo ratio and desulfurization activity, or the importance of ligand and ensemble effects. Our DFT calculations reveal that metcar Mo_8C_{12} bonds SO_2 as strongly as Mo_2C despite the high C/Mo ratio and C_2 groups. Spontaneous S−O bond cleavage occurs and the decomposition products interact simultaneously with *Mo and C*. The Mo_8C_{12} nanoparticle has a special chemical activity toward SO_2 as a result of its structure and an unexpected ligand effect. However, weak interactions are seen between Mo_8C_{12} and thiophene. Our results illustrate the complex behavior that a nanoparticle can have in desulfurization reactions.

II. Theoretical Section

The DMol³ code[38] was employed in the present study. It allows modeling the electronic structure and energetics of molecules, solids, and surfaces using DFT.[5,33,38,39] Following previous theoretical investigations,[30−32] we performed spin-restricted calculations. Here, all the electrons of C, O, S, H, and Mo were included in the calculations explicitly. The linear combinations of localized numerical atomic orbitals used as basis sets are designed to give maximum accuracy for a given basis set size.[38] In the present DMol³ calculations, we used a numerical basis set that describes the orbitals in the valence shell with double numerical functions (for example, Mo: 1s 2s 2p 3s 3p 3d 4s 4p 4d 5s 5p 4d′ 5s′ 5p′) and includes a polarization d-function for the light atoms (for example, C: 1s 2s 2p 2s′ 2p′ 3d). It is comparable in accuracy to a Gaussian 6-31G(d) basis set. A local basis cutoff of 5.5 Å in real space was employed. When a more extended basis set and a higher cutoff were tested, no remarkable changes occurred. Since the numerical basis set used here is of very high quality,[38] the basis set superposition error (BSSE) should be comparable for molecules and solids, and on the order of <10% of the reported bonding energies.[5,33,38b,39] The generalized gradient approximation (GGA) with the revised version of the Perdew−Burke−Ernzerhof functional (RPBE)[40] was utilized in the present work. The RPBE functional usually gives absolute errors in adsorption energy of ~0.2 eV.[5,33,40,41] Enough *k* points were selected (16) for the cases of the bulk α-Mo_2C(001) and δ-MoC(001) surfaces, making sure that there is no significant change in the calculated energies when a larger number of *k* points was used. In test calculations for S or O adsorption on δ-MoC(001) and TiC(001), we have found that DMol³ predicts bonding energies that are very similar to those obtained in DFT calculations with the CASTEP code (plane-wave basis set, with pseudopotentials to describe the core electrons).[32,41] For the SO_2/TiC(001) system, our theoretical approach gives a SO_2 adsorption energy of −0.63 eV,[5,41] which is close to the experimental observation of ca. ~−0.61 eV.[5] The first bond dissociation energy of a $Mo(CO)_6$ molecule, i.e., $Mo(CO)_6$ → $Mo(CO)_5$ + CO, calculated with DMol³ (1.63 eV) is in good agreement with the experimental value (1.73 eV).[42] As we will see below, similar good agreement is found between the predicted and measured adsorption energies for SO_2 and C_4H_4S on Mo_2C(001).

The adsorption of SO_2 and C_4H_4S was studied on both the metcar nanoparticle and bulk surfaces. In the present study, a series of possible adsorption sites for SO_2 and C_4H_4S was considered. A four-layer slab[32,41] was used to describe the α-Mo_2C(001) and δ-MoC(001) surfaces with a 4 × 2 unit cell on each layer, corresponding to 1/8 ML coverage. In the calculations, both the adsorbates and the metcar were allowed to relax in all dimensions. For the bulk surfaces, the top three
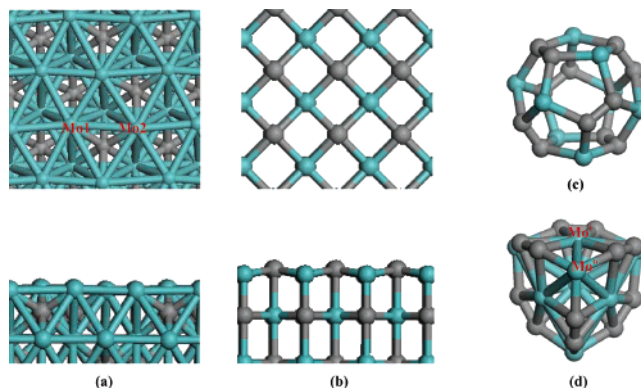
Figure 1. Optimized configurations of a α-Mo_2C(001) surface (a), a δ-MoC(001) surface (b), and metcar Mo_8C_{12} in T_h (c) and T_d (d) symmetry. Cyan and gray balls represent Mo and C atoms, respectively. For the bulk systems, at the top is shown a top view of the surface, and at the bottom a side view.

layers relaxed along with the adsorbates, while only the bottom layer was kept fixed at the calculated bulk lattice positions. All the geometries in the present study were optimized with no symmetry constraints. The calculated molecule adsorption energy was expressed as

$$E_{ads} = E(molecule/carbide) - E(carbide) - E(molecule) \tag{1}$$

In addition, for each optimized structure, a Mulliken population analysis[43a] was carried out to estimate the partial charge on each atom and examine *qualitative trends* in charge redistribution. When using the Mulliken method, one has to be careful with the type of basis set used.[43b,c] The basis set employed here and the Mulliken analysis give charge distributions for Mo_8C_{12} that are close to those derived from fitting electrostatic potentials with grid-based methods.[31,32]

III. Results and Discussion

In this section we will first briefly introduce the geometries of α-Mo_2C(001), δ-MoC(001), and Mo_8C_{12}, and then present and discuss the energetics for SO_2 and C_4H_4S adsorption and dissociation on the Mo carbide substrates.

III.1. Geometries of the Molybdenum Carbides. The α-phase of Mo_2C was found to have an orthorhombic crystal structure with the Mo atoms slightly distorted from their positions in close-packed planes and carbon atoms occupying ordered positions in lattice octahedral vacancies.[44] The DFT-RPBE calculated lattice constants for bulk α-Mo_2C are a = 4.819 Å, b = 6.012 Å, and c = 5.150 Å,[32] which are close to the experimental values.[45] The structure of α-Mo_2C perpendicular to the [001] direction (Figure 1a) includes a series of alternating Mo and C layers. Ideally, there are two kinds of Mo atoms in the Mo-terminated surface: Mo having one C atom coordination (Mo1, Figure 1a) and Mo having two C atoms coordination (Mo2, Figure 1a).
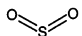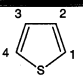
The δ-phase of MoC is the analogue of the well-known NaCl structure with a fcc Bravais lattice. The DFT-RPBE calculated lattice constant for bulk δ-MoC is 4.36 Å.[32] A value of 4.33 Å was measured experimentally.[46] According to our calculations, δ-MoC(001) has a surface configuration similar to that of TiC-(001).[33] The C atoms in a δ-MoC(001) surface move slightly outward and the Mo atoms inward, leading to a considerable zigzag effect (Figure 1b).

It has been found that the Mo_8C_{12} neutral or ion is particularly stable in the gas phase.[47] The structure of Mo_8C_{12} was originally
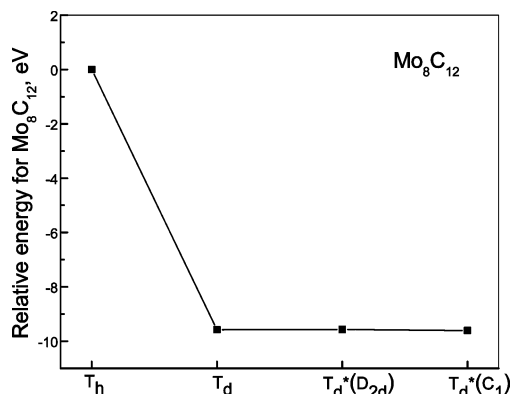
Figure 2. Relative stability for the T_h, T_d, and near-T_d (D_{2d} and C_1) structures of Mo_8C_{12}. The energies were calculated with DMol^3.

TABLE 1: Calculated and Experimental Geometries for SO_2 and C_4H_4S in the Gas Phase[a]

	SO_2 (gas)		C_4H_4S (gas)	
	Calc	Exp	Calc	Exp
S-O (Å)	1.49 (1.48[51])	1.43[48]	-	-
θ(O-S-O) (°)	120.1 (117.7[51])	119.3[48]	-	-
S-C$_1$ (Å)	-	-	1.74 (1.72,[52] 1.71[53])	1.71,[49] 1.71[50]
C$_1$-C$_2$ (Å)	-	-	1.38 (1.35,[52] 1.37[53])	1.37,[29] 1.37[50]
C$_2$-C$_3$ (Å)	-	-	1.43 (1.44,[52] 1.40[53])	1.43,[49] 1.40[50]
θ(C$_1$-S-C$_4$) (°)	-	-	91.6 (91.3,[52] 92.5[53])	92.2,[49] 92.5[50]

[a] Reference 51: B3LYP/6-31+G*. Reference 52: RHF/6-311++G**. Reference 53: DFT/GGA-PW91.

proposed as a pentagonal dodecahedral with T_h symmetry (Figure 1c).[47a] Shortly after, a restricted Hartree–Fock (RHF) study showed that Mo_8C_{12} adopted a tetrahedral structure with T_d symmetry (Figure 1d) instead of T_h symmetry.[30] Our recent spin-restricted DFT calculations using different functionals and basis sets indicate that T_d or slightly distorted T_d-like structures (D_{2d} and C_1) are much more stable than the T_h structure by almost 10 eV (see Figure 2 for DMol^3 results).[31,32a] The T_d structure for Mo_8C_{12} is based on a Mo_8 tetracapped tetrahedron (Figure 1d). Eight Mo atoms occupy two different positions: four high-coordinated inner atoms (Mo^i), and four low-coordinated outer atoms (Mo^o). DMol^3 predicts a very small energy separation between the T_d and T_d-like structures (D_{2d} and C_1) of Mo_8C_{12}, see Figure 2. Our calculations show that these T_d and T_d-like structures have a similar chemical reactivity.

III.2. Reactivity of Molybdenum Carbides toward SO_2 and C_4H_4S. The calculated geometries for the molecules SO_2 and C_4H_4S in the gas phase are listed in Table 1. The predicted geometries are in reasonable agreement with the experiments[48–50] and other theoretical studies.[16,51–53]

III.2.1. SO_2 Adsorption and Dissociation on Molybdenum Carbides. SO_2 adsorption on pure metal surfaces,[6a–c] alloy surfaces,[6d,e] and metal oxide surfaces[4,6f–h] has been extensively studied with both experiment and theory. According to these studies, SO_2 decomposes on most metal surfaces below 200 K,[6a–c] and only bonds weakly with the metal oxide surfaces.[4b–d,6f–h] Recently, a set of photoemission experiments observed the decomposition of SO_2 on the TiC(001) surface at temperatures of 300–400 K, a phenomenon well described by our DFT calcualtions.[5] Photoemission (PE) and X-ray absorption near-edge spectroscopy (XANES) have been used to examine the interaction of SO_2 with carbide-modified Mo(110) and

powders of bulk Mo_2C, observing S–O bond cleavage at temperatures below 150 K.[29] It seems that Mo_2C is as efficient as the pure metal toward S–O bond cleavage. However, no theoretical analysis has been performed for the SO_2/Mo_2C system. There has been no report regarding the activity of Mo_8C_{12} and MoC toward SO_2.

SO_2 was bonded to α-Mo_2C(001), δ-MoC(001), and Mo_8C_{12} through the S atom and two O atoms (η^3 bonding), the S atom and one O atom or two O atoms (η^2 bonding), and the S atom or a O atom (η^1 bonding). For all these configurations, we found that SO_2 prefers to bond to Mo sites instead of C sites of the carbide substrates. In the following paragraphs, the "η^α-S(O)$_\beta^\gamma$" notation is used to label the bonding configuration. "α" corresponds to the number of atoms of the adsorbate coordinated to the substrate. The atoms following the dash are the coordinated atoms. The subscript "β" stands for the coordination of the adsorption sites. For adsorption at the atop, bridge, or hollow site, "β" is expressed as "a", "b", or "h" accordingly. To describe the bonding on the metcar, a superscript "γ" is also included. In these cases, the "o" or "i" superscript means that an atom is coordinated to the outer or inner Mo atoms of the metcar, respectively. For example, a "η^3-S$_a^i$O$_a^o$O$_a^o$" label for SO_2/Mo_8C_{12} corresponds to an adsorbate configuration in which SO_2 interacts with Mo_8C_{12} through an S atom bonded to a Mo^i atom and two O atoms coordinated to two Mo^o atoms. Geometries that involve dissociation of the molecule are marked with the "*" symbol.

We start with SO_2 adsorption on the α-Mo_2C(001) surface to compare our calculations with the experiments.[29] The C/Mo ratio of Mo_2C is only 0.5 and all surface sites are occupied by Mo atoms (Figure 1a). Therefore, ensemble effects do not contribute in this case (i.e. no dilution of the number of Mo sites in the surface by C atoms). Six different configurations were considered for the SO_2/Mo_2C(001) system (Figure 3), which range from η^3 bonding to η^1 bonding. The results of the DFT calculations presented in Table 2 show that there is a very strong interaction between SO_2 and the α-Mo_2C(001) surface. For the strongest bonding configuration, there is spontaneous dissociation of the molecule: $SO_{2,gas} \rightarrow S_{ads} + 2O_{ads}$ (η^3-$S_hO_hO_h$*, Figure 3a). The adsorption energy is about -7.03 eV. Thus, our calculations are consistent with the experimental observations.[29] Both indicate that the decomposition of SO_2 on Mo_2C surfaces is very easy.

By increasing the C/Mo ratio to 1, more electrons transfer from Mo to C (ligand effect)[24a,31–33] and the number of Mo sites of the surface decreases by 50% compared to α-Mo_2C(001) (ensemble effect). Five different configurations (Figure 4) were considered for SO_2/MoC(001). Similarly to the case of SO_2/TiC(001),[5] SO_2 has a weak interaction with the δ-MoC(001) surface. The largest SO_2 adsorption energy on δ-MoC(001) (η^3-$S_aO_aO_a$, Figure 4a) is only -0.36 eV. No spontaneous S–O bond cleavage is observed, and the stretching of the S–O bonds is also very small (Table 2). With the contribution of both ligand and ensemble effects, the activity of the bulk δ-MoC(001) surface toward SO_2 adsorption greatly decreases compared to that of α-Mo_2C(001).

Additional calculations show that the decomposition of SO_2 on the δ-MoC(001) surface [$SO_{2,ads}$ (η^3-$S_aO_aO_a$, Figure 4a) $\rightarrow$ $S_{ads} + 2O_{ads}$] is highly exothermic ($\Delta E = -2.25$ eV), but the initial elongation of the S–O bonds requires surmounting an activation barrier of at least 0.4 eV as determined from partial geometry optimization. Therefore, we estimate that SO_2 could fully dissociate on a bulk δ-MoC(001) surface by thermal activation as seen in the case of TiC(001).[5] Our calculations
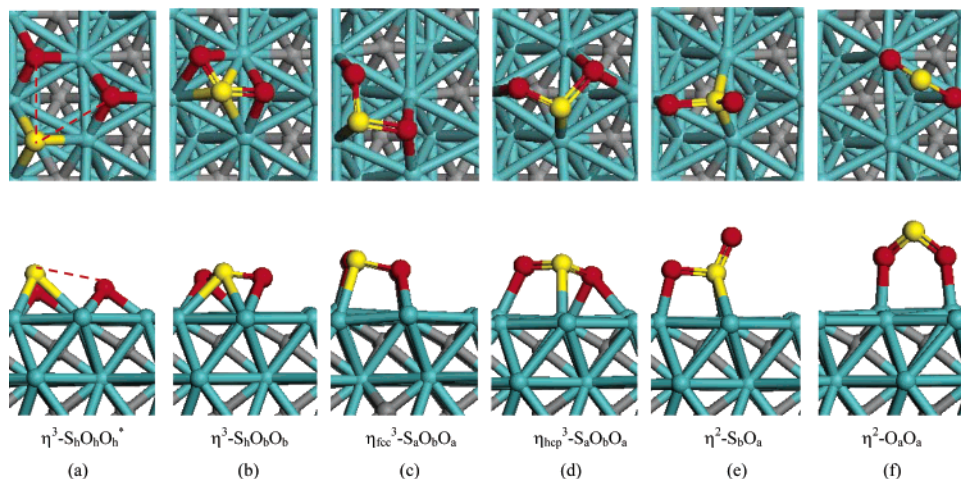
Figure 3. Configurations for SO$_2$ adsorption on a α-Mo$_2$C(001) surface (up: the top view; bottom: the side view). Subscripts "fcc" and "hcp" indicate that the center of SO$_2$ is located above the fcc or hcp sites in the surface, respectively. A dashed line stands for a broken bond. The symbol "*" denotes a dissociated configuration. Cyan and gray balls represent Mo and C atoms, respectively. Yellow and red balls correspond to sulfur and oxygen, respectively.

TABLE 2: Calculated Energetic and Geometric Parameters for SO$_2$ Adsorption on Mo Carbides[a]

|			ΔE_{ads} (eV)	d(S–O) (Å)	d(O–Mo) (Å)	d(S–Mo) (Å)	θ(O–S–O) (deg)
Mo$_2$C(001)	η^3-S$_h$O$_h$O$_h$*		−7.04	3.19	2.09	2.44	58.7
	η^3-S$_h$O$_b$O$_b$	$\Rightarrow \eta^3$-S$_h$O$_h$O$_h$*					
	η_{fcc}^3-S$_a$O$_b$O$_a$		−2.60	1.73	2.17	2.47	104.6
	η_{fcc}^3-S$_a$O$_a$O$_a$	$\Rightarrow \eta_{fcc}^3$-S$_a$O$_b$O$_a$					
	η_{hcp}^3-S$_a$O$_b$O$_a$		−2.47	1.62, 1.77	2.56, 2.31	2.47	106.0
	η_{hcp}^3-S$_a$O$_a$O$_a$	$\Rightarrow \eta_{hcp}^3$-S$_a$O$_b$O$_a$					
	η^2-S$_b$O$_a$		−2.35	1.50, 1.69	2.06	2.41	109.2
	η^1-S$_b$	$\Rightarrow \eta^2$-S$_b$O$_a$					
	η^2-O$_a$O$_a$		−1.87	1.61	2.08		108.9
MoC(001)	η^3-S$_a$O$_a$O$_a$		−0.36	1.59	2.35	2.62	113.1
	η^2-O$_a$O$_a$		−0.28	1.56	2.25		115.6
	η^1-S$_a$		−0.27	1.49		2.47	119.7
	η^1-S$_b$		−0.02	1.49			119.9
Mo$_8$C$_{12}$	η^3-S$_a^i$O$_b^o$O$_b^o$*		−2.93	4.36	2.17	2.34	43.8
	η^3-S$_a^i$O$_a^o$O$_a^o$	$\Rightarrow \eta^3$-S$_a^i$O$_b^o$O$_b^o$*					
	η^2-O$_a^o$O$_a^o$		−1.56	1.62	2.16	2.87	96.1
	η^1-O$_a^o$		−1.36	1.62, 1.52	2.02	3.48	114.0
	η^1-S$_a^o$		−1.29	1.49	3.37	2.37	120.0
	η^2-O$_a^i$O$_a^o$		−1.07	1.63, 1.57	2.32, 2.08	3.23	113.5
	η^2-S$_a^i$O$_a^o$		−0.72	1.62, 1.51	2.15	2.65	112.7
	η^1-S$_a^i$		−0.61	1.49		2.41	118.3

[a] The symbol "*" denotes a dissociated configuration.

also indicate that the dissociated O and S adatoms prefer the pseudohollow sites constructed by two Mo atoms *and one C atom* instead of Mo atop sites. With O and S adatoms bonded only to Mo sites, it was found that the energy of dissociation [SO$_{2,ads}$ (η^3-S$_a$O$_a$O$_a$, Figure 4a) → S$_{ads}$ + 2O$_{ads}$] becomes ca. −0.36 eV. Therefore, the participation of the surface C sites in the reaction plays an essential role in the energetics of SO$_2$ dissociation on this metal carbide surface. This is a very interesting result, since in desulfurization studies on molybdenum carbide it is usually assumed[23,24,27b,29] that the C sites are simple spectators. Our calculations are consistent with PE experiments for adsorption of SO$_2$ on carbide-modified Mo(110),[29] which show a significant broadening of the C 1s peak upon decomposition of the adsorbate (C↔S and C↔O interactions).

Because of the six C$_2$ groups, the C/Mo ratio of the metcar Mo$_8$C$_{12}$ is as high as 1.5. As compared with the case of MoC, highly symmetric Mo sites (Figure 1) also disappear (ensemble effect), but the electron transfer from Mo to C (ligand effect) can be less due to weaker Mo↔C interactions (C–C bonding weakens Mo–C bonds).[31–33] For SO$_2$ adsorption on Mo$_8$C$_{12}$,

eight different configurations were taken into consideration in the present study (Figure 5). As shown in Table 2, our DFT calculations indicate that Mo$_8$C$_{12}$ interacts strongly with SO$_2$, like α-Mo$_2$C does. Thus, starting from a η^3-S$_a^i$O$_a^o$O$_a^o$ configuration (Figure 5b) we observe a spontaneous dissociation of SO$_2$ on Mo$_8$C$_{12}$ [SO$_{2,gas}$ → η^3-S$_a^i$O$_b^o$O$_b^o$* (Figure 5a), ΔE = −2.93 eV] during the geometry optimization. It is the most stable structure for SO$_2$/Mo$_8$C$_{12}$. In addition, we also notice that the dissociated O adatoms occupy Mo^o–C bridge sites (η^3-S$_a^i$O$_b^o$O$_b^o$*, Figure 5a) instead of the Mo^o atop sites. As to the C atoms in the δ-MoC(001) surface, the C$_2$ groups of the metcar contribute to the desulfurization reaction by stabilizing the S or O adatoms. Most importantly, it seems that the high C/Mo ratio of the metcar and its C$_2$ groups may greatly increase the stability of this molecule[30–33] with only a relatively small decrease in its reactivity toward SO$_2$. No significant deactivation is found like in the case of δ-MoC(001) where the SO$_2$ molecule does not dissociate spontaneously.

On the basis of our extensive DFT calculations, we now take a step further to analyze the ligand and ensemble effects of C
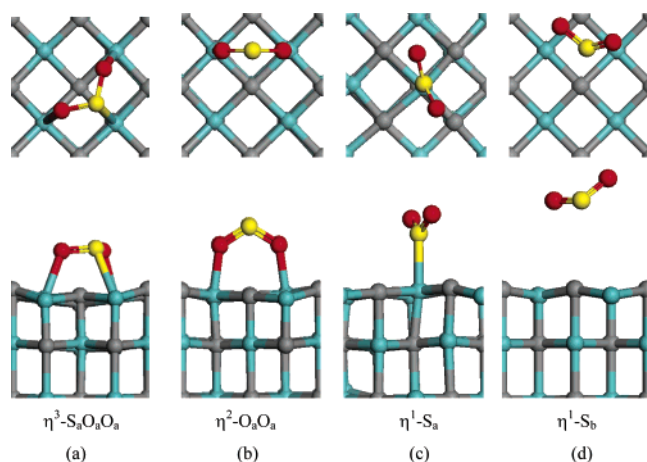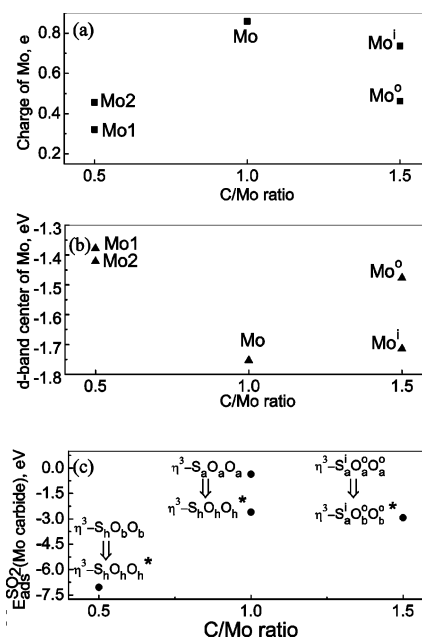
Figure 4. Configurations for SO_2 adsorption on a δ-MoC(001) surface (up: the top view; bottom: the side view). Cyan and gray balls represent Mo and C atoms, respectively. Yellow and red balls correspond to sulfur and oxygen, respectively.
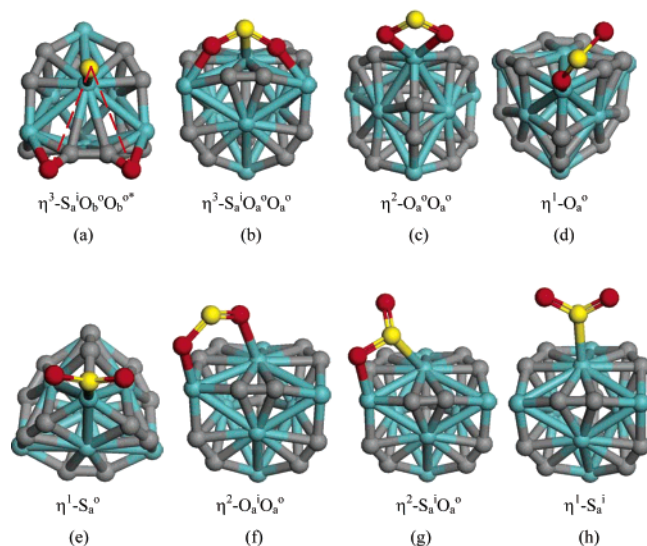
Figure 5. Configurations for SO_2 adsorption on metcar Mo_8C_{12} in a T_d-like C_1 symmetry. The dashed line stands for the broken bond. The symbol "*" denotes a dissociated configuration. Cyan and gray balls represent Mo and C atoms, respectively. Yellow and red balls correspond to sulfur and oxygen, respectively.

on the reactivity of Mo toward SO_2. By increasing the C concentration in a carbide, the electronic structure of Mo atoms changes (ligand effect)[54] due to a substantial electron transfer from Mo to C (Figure 6a).[31-33] The Mo atoms in a δ-MoC-(001) surface are more positively charged by ~0.4e than those of α-Mo_2C(001). In contrast, the charge difference between low-coordinated Mo^o atoms of Mo_8C_{12} and Mo atoms of α-Mo_2C-(001) is only ~0.1e. The position of the d-band center of a Mo atom, which affects its chemical activity,[35] inversely changes with an increasing C/Mo ratio (Figure 6b). The more positively charged the Mo atoms, the lower their d-band center and therefore lower their chemical activity. Thus, in the case that a ligand effect is overwhelming, Mo_8C_{12} may behave similar to α-Mo_2C despite the high C/Mo ratio and C_2 groups. Increasing the C concentration, on the other hand, decreases the number of active Mo sites that can be exposed on the surface, and should greatly deactivate Mo_8C_{12} if such an ensemble effect dominates the chemistry of adsorbed SO_2.

Figure 6c plots the calculated SO_2 adsorption energy for the most stable configurations on α-Mo_2C(001), δ-MoC(001), and Mo_8C_{12} as a function of the C/Mo ratio. One can see that the


Figure 6. Charge on Mo atoms (a), the position of the d-band center of the Mo atoms (b), and the SO_2 adsorption energy (c) for the carbides as a function of the C/Mo ratio: 0.5 for Mo_2C, 1.0 for MoC, and 1.5 for Mo_8C_{12}. The symbol "*" denotes a dissociated configuration.

Mo carbides at low C/Mo ratio (α-Mo_2C) and high C/Mo ratio (Mo_8C_{12}) are very reactive toward SO_2 and both lead to spontaneous cleavage of the S–O bonds. SO_2 molecules adsorb weakly on a δ-MoC(001) surface by only occupying Mo sites which have a d-band shifted downward (ligand effect, Figure 6). With the participation of the active C atoms of the surface, the full dissociation of SO_2 on the carbide becomes a highly exothermic process. Yet, it needs thermal activation and eventually there should be a competition with desorption of the admolecule.[5a] With the d-band position of Mo^o located closer to the Fermi level than those in δ-MoC(001), the cleavage of S–O bonds on the Mo_8C_{12} nanoparticle becomes a nonactivated reaction. Thus, it seems that a ligand effect is responsible for the high activity of the Mo_8C_{12} nanoparticle toward SO_2 (Figure 6b). Thus, a high C/Mo ratio does not necessarily imply a low desulfurization activity when dealing with a carbide nanoparticle.

Our calculations also show that the behavior of SO_2 on the molybdenum carbide substrates has a lot in common with that found for the molecule on metals and alloys.[6] First, there is a substantial perturbation of the molecular geometry with an elongation of the S–O bonds and a contraction of O–S–O bond angle. Second, the most stable configurations for adsorbed SO_2 involve η^2 or η^3 bonding. And third, the adsorbed SO_2 dissociates into S and O adatoms. According to our results, the metal carbides are more efficient than metal oxides[4b-d,6g,55] for the destruction of SO_2. In the case of metal oxide surfaces, the cations have a very low electron density and interact weakly with the SO_2 molecule.[4c,6g] There is no dissociation of the S–O bonds and the main sulfur species present on the oxides are SO_3 or SO_4 groups ($SO_{2,gas} + nO_{oxide} \rightarrow SO_{2+n,ads}$).[4b-d,6g,55]

III.2.2. Thiophene Adsorption and Dissociation on Molybdenum Carbides. Thiophene is a typical probe molecule in hydrodesulfurization studies.[2,26,27] Previous works have been focused on the interaction of the C_4H_4S molecule with transition metals,[3,8-11] alloys,[15,18-20] oxides,[56-58] sulfides,[2b,13,16,17,21] nitrides,[12,22] and carbides as well.[17,23] The bonding and chemistry of C_4H_4S on metal surfaces has been studied in detail.[8-11] Although metal carbides have a high activity in HDS reactions,[24,25] so far there have been only two experimental studies
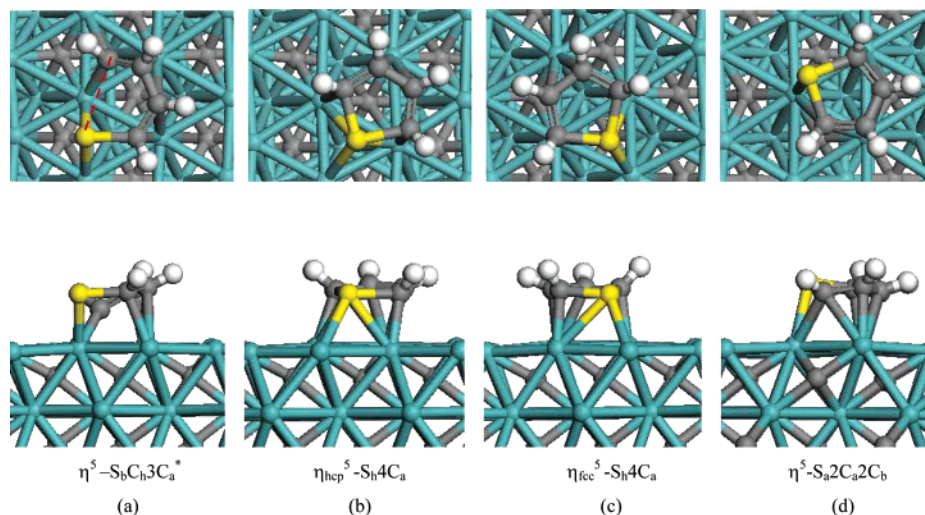
Figure 7. Configurations for C$_4$H$_4$S adsorption on a α-Mo$_2$C(001) surface (up: the top view; bottom: the side view). Subscripts "fcc" and "hcp" represent that the ring of C$_4$H$_4$S is located above fcc or hcp hollow sites in the surface, respectively. The dashed line stands for the broken bond. The symbol "*" denotes a dissociated configuration. Cyan balls represent Mo. Gray balls stand for carbon. Yellow, red, and white balls correspond to sulfur, oxygen, and hydrogen, respectively.

TABLE 3: Calculated Energetic and Geometric Parameters for C$_4$H$_4$S Adsorption on Mo Carbides[a]

			ΔE_{ads} (eV)	d(S−C) (Å)	d(S−Mo) (Å)	d(C−Mo) (Å)	θ(C$_1$−S−C$_4$) (deg)
Mo$_2$C(001)	η^5-S$_b$2C$_b$C$_a$*		−2.74	2.94, 1.83	2.49	2.21∼2.36	89.6
	η^5-S$_b$2C$_b$2C$_a$	$\Rightarrow \eta^5$-S$_b$C$_h$3C$_a$*					
	η_{hcp}^5-S$_h$4C$_a$		−1.77	1.86,1.92	2.63∼2.76	2.19∼2.56	93.2
	η_{fcc}^5-S$_h$4C$_a$		−1.74	1.85	2.54∼2.80	2.18∼2.54	96.0
	η^5-S$_a$2C$_a$2C$_b$		−1.51	1.84,1.86	2.51	2.21∼2.63	91.6
	η^5-S$_a$4C$_a$	$\Rightarrow \eta^5$-S$_a$2C$_a$2C$_b$					
	η^1-S$_b$	$\Rightarrow \eta^5$- S$_h$4C$_a$					
MoC(001)	η^5-S$_a$4C$_a$		−0.30	1.79	2.60	2.35∼2.39	93.7
	η^5-S$_b$4C$_a$		−0.17	1.77	2.61	2.42∼2.44	91.3
	η^1-S$_a$		>0	1.74	4.02		91.8
Mo$_8$C$_{12}$	η^1-S$_a$^{o}		−0.60	1.75	2.47	3.86	92.8
	tilted η^1-S$_a$^{o}		−0.58	1.76	2.61	3.55	91.5
	η^3-S$_a$^{o}2C$_a$^{o}		−0.46	1.80	2.48	2.38	85.3
	η^5-S$_a$^{o}4C$_a$^{o}	$\Rightarrow \eta^3$-S$_a$^{o}2C$_a$^{o}					
	tilted η^1-S$_a$^{i}		−0.29	1.75	2.76	3.79	91.8
	η^5-S$_a$^{i}4C$_a$^{i}	$\Rightarrow$ tilted η^1-S$_a$^{i}					
	η^1-S$_a$^{i}		−0.20	1.74	2.70	4.02	93.0
	η^2-S$_a$^{o}C$_a$^{i}		−0.01	1.74	4.67	4.28	91.8

[a] The symbol "*" denotes a dissociated configuration.

examining the adsorption of C$_4$H$_4$S on carbide surfaces (carbide-modified Mo(110)[17] and α-Mo$_2$C(001)[23]). It was observed that the decomposition of thiophene on both surfaces occurred at temperatures below ∼200 K. C$_4$H$_4$S adsorption on the metcar Mo$_8$C$_{12}$ or the δ-MoC(001) surface has not been investigated.

C$_4$H$_4$S can bond to a surface via either its π-system (η^5) or the lone pair of electrons associated with the S atom (η^1).[2b,3,10,61] In the current study, a "η^α-Sn(C)$_\beta^\gamma$" notation is used to label the different bonding configuration for adsorbed C$_4$H$_4$S. The superscripts (α,γ) and subscript (β) have the same meaning as in the case of SO$_2$ adsorption. In addition, the integer "n" represents the number of C atoms that occupy the same kind of sites. The default value of n is 1.

Since there are experimental data for the interaction of C$_4$H$_4$S with α-Mo$_2$C(001),[23] we will begin by examining this system theoretically. To find the most stable structure for the adsorbed C$_4$H$_4$S on a α-Mo$_2$C(001) surface, one upright (η^1-S) and five flat (see Figure 7) configurations were considered and fully relaxed. The η^1-S configuration transformed into a flat configuration (Figure 7c) during the geometry optimization. Table 3 summarizes the structural parameters and adsorption energies for the bonding of C$_4$H$_4$S to α-MoC(001). According to our results, the molecule interacts strongly with this carbide surface.

In one of the planar configurations, a C−S bond spontaneously breaks and all four C atoms form strong bonds with Mo atoms of the surface (η^5-S$_b$2C$_b$2C$_a$ → η^5-S$_b$C$_h$3C$_a$*, Figure 7a). This is the most stable configuration and corresponds to an adsorption energy of −2.74 eV. The present calculations also show that the successive scission of the other C−S bond releases an extra energy of 1.18 eV (η^5-S$_h$2C$_h$2C$_a$*, a-III, Figure 8). Such a phenomenon is also observed when C$_4$H$_4$S is adsorbed on metal surfaces,[10] but not when the molecule interacts with sulfides[2b,21] or oxides.[56−58] Thus, our calculations are in reasonable agreement with the PE experiments.[23] Both indicate that the dissociation of C$_4$H$_4$S on a α-Mo$_2$C(001) surface is a relatively facile reaction. The behavior of C$_4$H$_4$S on α-Mo$_2$C(001) has a lot in common with that found on transition metals.[3,8−11] Flat adsorption structures (η^5-bonding) are found to be more stable than upright ones, and there is cleavage of C−S bonds.

For C$_4$H$_4$S adsorption on a δ-MoC(001) surface, three different kinds of geometries were taken into consideration, as shown in Figure 9. According to the results in Table 3, on this carbide surface the adsorbate also prefers η^5 bonding (η^5-S$_a$-4C$_a$, Figure 9a) rather than η^1 bonding (η^1-S$_a$, Figure 9c), but overall the C$_4$H$_4$S molecule adsorbs very weakly. The most stable bonding configuration (η^5-S$_a$4C$_a$) corresponds to an
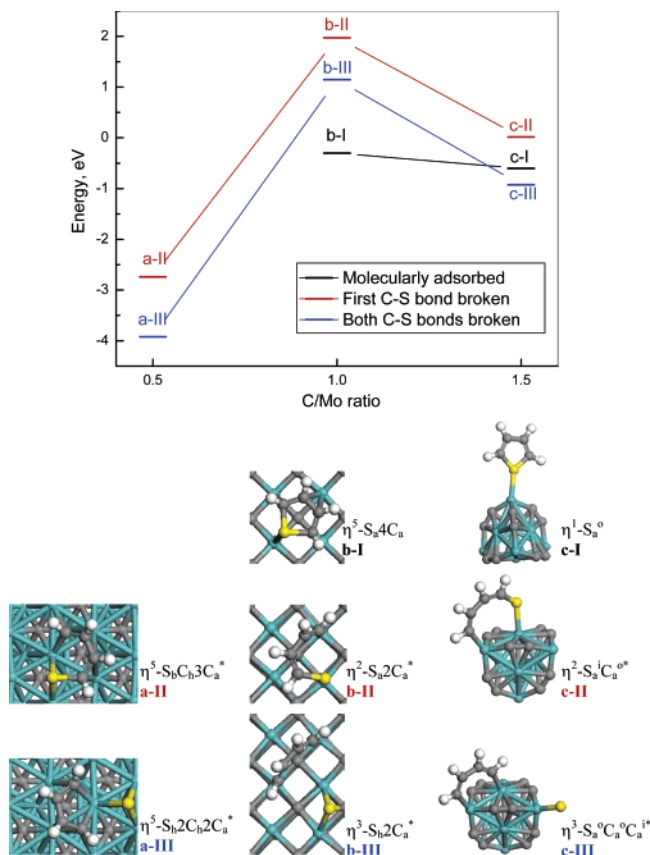
Figure 8. Energy changes associated with the desulfurization of C_4H_4S on Mo carbides. Starting from a molecularly adsorbed configuration (I), the desulfurization process involves the successive scission of two C−S bonds (II and III). The C/Mo ratios with a value of 0.5, 1, and 1.5 correspond to $Mo_2C(001)$, $MoC(001)$, and Mo_8C_{12}, respectively. The energies shown in the figure are relative to a free C_4H_4S molecule and clean Mo carbide systems. The symbol "*" denotes a dissociated configuration. Cyan balls represent Mo. Gray balls stand for carbon. Yellow, red, and white balls correspond to sulfur, oxygen, and hydrogen, respectively.
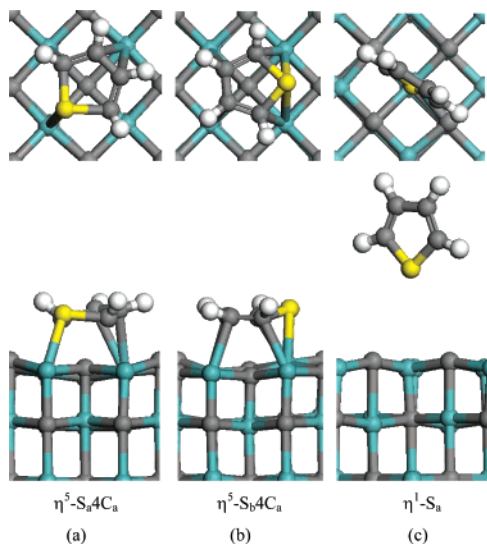
Figure 9. Configurations for C_4H_4S adsorption on a δ-MoC(001) surface (up: the top view; bottom: the side view). Cyan balls represent Mo. Gray balls stand for carbon. Yellow, red, and white balls correspond to sulfur, oxygen, and hydrogen, respectively.

adsorption energy of only −0.3 eV, which is about nine times smaller than that of C_4H_4S on α-$Mo_2C(001)$. Furthermore, the molecule adsorbed on δ-MoC(001) has almost the same
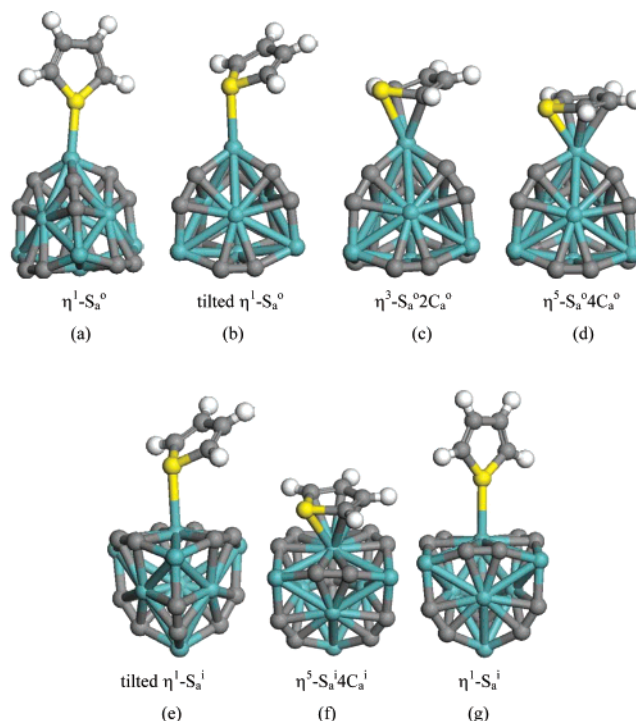
Figure 10. Configurations for C_4H_4S adsorption on metcar Mo_8C_{12} in a T_d-like C_1 symmetry. Gray balls stand for carbon. Yellow, red, and white balls correspond to sulfur, oxygen, and hydrogen, respectively.

interatomic distances as in the gas phase (Table 1). The dissociation of C_4H_4S on δ-MoC(001) by breaking a C−S bond (η^5-S_a4C_a, Figure 9a, to η^2-S_aC_a*, Figure 8) is a highly endothermic process ($\Delta E = 1.98$ eV). The breaking of two C−S bonds (η^5-S_a4C_a, Figure 9a, to η^3-S_h2C_a*, Figure 8) is also an uphill reaction ($\Delta E = 1.14$ eV). Thus, it seems that C−S bond cleavage on δ-MoC is almost impossible. As compared to α-$Mo_2C(001)$, δ-MoC(001) is deactivated due to both ligand (a substantial electron transfer from Mo to C, Figure 6) and ensemble (missing of pure Mo sites with high symmetry) effects.[30−32] In addition, the C atoms in the ridge of the rippled δ-MoC(001) surface (Figure 1b) may prevent the thiophene molecule from approaching the surface (steric effect). Therefore, the S and C atoms in particular cannot form strong short bonds with Mo atoms.

Now we turn to the Mo_8C_{12} nanoparticle. The geometries for C_4H_4S adsorption on Mo_8C_{12} are more complicated because of its unique structure. Eight configurations were considered including parallel, tilted, and upright bonding modes (Figure 10). Our calculations indicate that, unlike the case of SO_2, the metcar nanoparticle has a low reactivity toward C_4H_4S and behaves almost as inert as δ-MoC. The strongest adsorption energy of C_4H_4S on Mo_8C_{12} is only −0.6 eV (η^1-S_a^o) and the interatomic distances of the molecule are only slightly stretched (Table 3). The results also show that a geometry for thiophene with one C−S bond broken (η^2-$S_a^iC_a^o$*, Figure 8) is less stable by ~0.6 eV than that of molecularly adsorbed C_4H_4S (Figure 10a). The scission of two C−S bonds on the metcar (η^3-$S_a^oC_a^oC_a^i$*, Figure 8) is slightly favored in energy as compared to the molecularly adsorbed state by 0.32 eV. The reaction energy of $C_4H_4S + Mo_8C_{12} \rightarrow \eta^3$-$S_a^oC_a^oC_a^i$* is nearly −1 eV (Figure 8), but the desulfurization process is made difficult by the endothermicity associated with the cleavage of the first C−S bond.

Table 3 indicates that on Mo_8C_{12}, bonding configurations of C_4H_4S with a high coordination (η^5 or η^3) are not as stable as

Desulfurization of SO₂ and Thiophene

J. Phys. Chem. B, Vol. 108, No. 40, 2004 **15669**

those with a simple η^1 coordination through the S atom. This behavior is completely different from that seen on the α-Mo₂C-(001) and δ-MoC(001) surfaces. Due to the high C/Mo ratio, Mo₈C₁₂ cannot provide a set of Mo sites such as a α-Mo₂C-(001) substrate (ensemble effect). But, in principle, each face of Mo₈C₁₂ exposes four Mo sites (Figure 1d) that could bond thiophene well in a η^5 or η^3 configuration. The reasonably high activity of these sites for the adsorption (ligand effect) should be observed as well documented for the dissociation of SO₂ (Table 2). Steric effects are probably responsible for the low reactivity of Mo₈C₁₂ toward thiophene. The C₂ groups of the metcar move outward with respect to the Mo sites (Figure 1d) and block interactions with C₄H₄S in η^3 or η^5 configurations and with the C₄H₄ fragment produced by desulfurization of the adsorbate. It is interesting to notice in Table 3 that, even with a steric repulsion between the C₂ groups and thiophene, the Mo₈C₁₂ nanoparticle interacts with this molecule a little better than with the δ-MoC(001) surface ($\sim$0.3 eV).

Recent theoretical works that deal with the chemical properties of pure metal nanoparticles highlight the importance of corner or edge sites.[59-62] Our results show that the situation can be more complex in the case of a metal compound. A carbide nanoparticle can have a high chemical activity, due to not only the presence of corner or edge sites but also the adoption of stoichiometries and geometries quite different from those of the bulk material. The special geometry of Mo₈C₁₂ attenuates the ligand effects of C on Mo, and the nanoparticle interacts well with small adsorbates such as SO₂, S,[32] or CO.[31,32] In this respect, a high carbon/metal ratio does not imply a low chemical or catalytic activity. When dealing with a large adsorbate, one must also consider the position of the nonmetal atoms in the nanoparticle. Steric repulsion can overcome the intrinsic reactivity of metal atoms in corner or edge sites.

IV. Conclusions

DFT calculations indicate that a α-Mo₂C(001) surface is very reactive toward SO₂ and thiophene, being able to spontaneously break S—O and S—C bonds. In this carbide system the ligand effects of C are minimal, and the Mo atoms have a desulfurization activity similar to that of the atoms in pure metal surfaces. δ-MoC(001) exhibits a low reactivity due to ligand and ensemble effects (high C/Mo ratio). SO₂ and C₄H₄S adsorb molecularly on δ-MoC(001) with bonding energies that are at least nine times smaller than those on α-Mo₂C(001). There is an activation barrier for the decomposition of SO₂ on δ-MoC-(001). Contrary to common assumptions, the C atoms are not simple spectators and play a key role in the energetics for the dissociation of SO₂.

The Mo₈C₁₂ nanoparticle is very reactive toward SO₂ despite the high C/Mo ratio and the C₂ groups. As in the case of α-Mo₂C(001), spontaneous cleavage of the S—O bonds is also feasible on Mo₈C₁₂. The particular geometry of the metcar attenuates the ligand effects of C on Mo and favors desulfurization reactions. With respect to the metal atoms in δ-MoC-(001), the Mo atoms in Mo₈C₁₂ have a smaller positive charge and a d-band center shifted upward. However, for C₄H₄S adsorption on the metcar, steric repulsion between the C₂ groups and thiophene can overcome the high reactivity of the Mo atoms in corner or edge sites. The behavior of Mo₈C₁₂ illustrates the interplay of ligand and steric effects in nanoparticles of metal compounds.

Note Added after ASAP Posting. This paper was published on Articles ASAP on September 2, 2004, with the words "low" and "high" transposed in the third sentence before section III.2. The corrected version was reposted on September 8, 2004.

References and Notes

(1) (a) Rodriguez, J. A.; Hrbek, J. *Acc. Chem. Res.* **1999**, *32*, 719. (b) Farrauto, R. J.; Bartholomew, C. H. *Fundamentals of Industrial Catalytic Processes*; Chapman and Hall: New York, 1997. (c) Stirling, D. *The Sulfur Problem*: *Cleaning Up Industrial Feedstocks*; Royal Society of Chemistry: Cambridge, UK, 2000.

(2) (a) Satterfield, C. N. *Heterogeneous Catalysis in Industrial Practice*; Mc-Graw Hill: New York, 1991. (b) Zonnevylle, M. C.; Hoffmann, R.; Harris, S. *Surf. Sci.* **1988**, *199*, 320.

(3) Liu, G.; Rodriguez, J. A.; Dvorak, J.; Hrbek, J.; Jirsak, T. *Surf. Sci.* **2002**, *505*, 295.

(4) (a) Pieplu, A.; Saur, O.; Lavalley, J. C.; Legendre, O.; Nedez, C. *Catal. Rev. Sci. Eng.* **1998**, *40*, 409. (b) Pacchioni, G.; Ricart, J. M.; Illas, F. *J. Am. Chem. Soc.* **1994**, *116*, 10152. (c) Pacchioni, G.; Clotet, A.; Ricart, J. M. *Surf. Sci.* **1994**, *315*, 337. (d) Schneider, W. F.; Li, W. F.; Hass, K. C. *J. Phys. Chem. B* **2001**, *105*, 6972.

(5) (a) Rodriguez, J. A.; Liu, P.; Dvorak, J.; Jirsak, T.; Gomes, J.; Takahashi, Y.; Nakamura, K. *Surf. Sci.* **2003**, *543*, L675. (b) Liu, P.; Rodriguez, J. A. *J. Chem. Phys.* **2003**, *119*, 10895.

(6) (a) Jirsak, T.; Rodriguez, J. A.; Hrbek, J. *Surf. Sci.* **1999**, *426*, 319. (b) Rodriguez, J. A.; Ricart, J. M.; Clotet, A.; Illas, F. *J. Chem. Phys.* **2001**, *115*, 454. (c) Haase, J. *J. Phys. Matter* **1997**, *9*, 3647 and references therein. (d) Rodriguez, J. A.; Jirsak, T.; Chaturvedi, S.; Hrbek, J. *J. Am. Chem. Soc.* **1998**, *120*, 11149. (e) Rodriguez, J. A.; Jirsak, T.; Chaturvedi, S. *J. Chem. Phys.* **1999**, *110*, 3138. (f) Rodriguez, J. A.; García, J.; González, L. *Chem. Phys. Lett.* **2002**, *365*, 380. (g) Rodriguez, J. A.; Jirsak, T.; González, L.; Evans, J.; Pérez, M.; Maiti, A. *J. Chem. Phys.* **2001**, *115*, 10914 and references therein. (h) Rodriguez, J. A.; Jirsak, T.; Freitag, A.; Larese, J. Z.; Maiti, A. *J. Chem. Phys.* **2000**, *104*, 7439 and references therein.

(7) Alemozafar, A. R.; Guo, A. C.; Madix, R. J. *Surf. Sci.* **2003**, *524*, L84.

(8) Terada, S.; Yokoyama, T.; Sakano, M.; Imanishi, A.; Kitajima, Y.; Kiguchi, M.; Okamoto Y.; Ohta, T. *Surf. Sci.* **1998**, *414*, 107.

(9) Milligan, P. K.; Murphy, B.; Lennon, D.; Cowie, B. C. C.; Kadodwala, M. *J. Phys. Chem. B* **2001**, *105*, 140.

(10) (a) Mittendorfer, F.; Hafner, J. *Surf. Sci.* **2001**, *492*, 27. (b) Morin, C.; Eichler, A.; Hirschl, R.; Sautet, P.; Hafner, J. *Surf. Sci.* **2003**, *540*, 474.

(11) Rousseau, G. B. D.; Bovet, N.; Johnston, S. M.; Lennon, D.; Dhanak. V.; Kadodwala, M. *Surf. Sci.* **2002**, *511*, 190.

(12) Wu, Z.; Li, C.; Wei, Z.; Ying, P.; Xin, Q. *J. Phys. Chem.* **2002**, *106*, 979.

(13) Rodriguez, J. A.; Dvorak, J.; Jirsak, T.; Hrbek, J. *Surf. Sci.* **2001**, *490*, 315.

(14) Da Costa, P.; Potvin, C.; Manoli, J.-M.; Breysse, M.; Djega-Mariadassou, G. *Catal. Lett.* **2003**, *86*, 133.

(15) Khan, N. A.; Hwu, H. H.; Chen, J. G. *J. Catal.* **2002**, *205*, 259.

(16) Smelyansky, V.; Hafner, J.; Kresse, G. *Phys. Rev. B* **1998**, *58*, R1782.

(17) Rodriguez, A.; Dvorak, J.; Jirsak, T. *Surf. Sci.* **2000**, *457*, L413.

(18) Vebezia, A. M.; La Parola, V.; Deganello, G.; Cauzzi, D.; Leonardi, G.; Predieri, G. *Appl. Catal. A* **2002**, *229*, 261. (b) Venezia, A. M.; La Parola, V.; Nicoli, V.; Deganello, G. *J. Catal.* **2002**, *212*, 56.

(19) Au, X. D.; Waller, P.; Crezee, E.; Shan, Z.; Kapteijn, F.; Moulijn, J. A. *Stud. Surf. Sci. Catal.* **2002**, *143*, 1019.

(20) Damyanova, S.; Petrov, L.; Grange, P. *Appl. Catal. A* **2003**, *239*, 241.

(21) (a) Rodriguez, J. A.; Dvorak, J.; Capitano, A. T.; Gabelnick, A. M.; Gland, J. L. *Surf. Sci.* **1999**, *429*, L462. (b) Rodriguez, J. A. *J. Phys. Chem. B* **1997**, *101*, 7524. (c) Tarbuck, T. L.; McCrea, K. R.; Logan, J. W.; Heiser, J. L.; Bussell, M. E. *J. Phys. Chem. B* **1998**, *102*, 7845. (d) Orita, H.; Uchida, K.; Itoh, N. *J. Mol. Catal. A: Chem.* **2003**, *193*, 197. (e) Paul, J. F.; Payen, E. *J. Phys. Chem. B* **2003**, *107*, 4057. (f) Aray, Y.; Rodríguez, J.; Vega, D.; Coll, S.; Rodríguez-Arias, E. N.; Rosillo, F. *J. Phys. Chem. B* **2002**, *106*, 13242. (g) Lee, J. J.; Kim, H.; Moon, S. H. *Appl. Catal. B* **2003**, *41*, 171. (h) Pettiti, I.; Botto, I. L.; Cabello, C. I.; Colonna, S.; Faticanti, M.; Minelli, G.; Porta, P.; Thomas, H. J. *Appl. Catal. A* **2001**, *220*, 113.

(22) Hada, K.; Tanabe J.; Omi, S.; Nagai, M. *J. Catal.* **2002**, *207*, 10.

(23) St. Clair, T. P.; Oyama, S. T.; Cox, D. F. *Surf. Sci.* **2002**, *511*, 294.

(24) (a) Chen, J. G. *Chem. Rev.* **1996**, *96*, 1447. (b) Furimsky, E. *Appl. Catal. A* **2003**, *240*, 1. (c) Oyama, S. T. *Catal. Today* **1992**, *15*, 179.

(25) Hugosson, H. W.; Jansson, U.; Johansson, B.; Eriksson, O. *Chem. Phys. Lett.* **2001**, *333*, 444.

(26) (a) Topsøe, H.; Clausen, B. S.; Massoth, F. E. *Catalysis, Science and Technology*; Springer: Berlin, Germany, 1996. (b) Byskov, L. S.; Hammer, B.; Nørskov, J. K.; Clausen, B. S.; Topsøe, H. *Catal. Lett.* **1997**, *47*, 177.

(27) (a) Chianelli, R. R.; Daage, M.; Ledoux, M. J. *Adv. Catal.* **1994**, *40*, 177. (b) Chianelli, R. R.; Berhault, G. *Catal. Today* **1999**, *53*, 357.

(28) Sajkowski, D. J.; Oyama, S. T. *Appl. Catal. A* **1996**, *134*, 339.

(29) Rodriguez, A.; Dvorak, J.; Jirsak, T. *J. Phys. Chem. B* **2000**, *104*, 11515.

(30) Lin, Z.; Hall, M. B. *J. Am. Chem. Soc.* **1993**, *115*, 11165.

(31) Hou, H.; Muckerman, J. T.; Liu, P.; Rodriguez, J. A. *J. Phys. Chem. A* **2003**, *107*, 9344.

(32) (a) Liu, P.; Rodriguez, J. A. *J. Chem. Phys.* **2004**, *120*, 5414. (b) Liu, P.; Rodriguez, J. A. *Catal. Lett.* **2003**, *91*, 247.

(33) Liu, P.; Rodriguez, J. A.; Hou, H.; Muckerman, J. T. *J. Chem. Phys.* **2003**, *118*, 7737.

(34) Chen, J. G. Private communication.

(35) (a) Greeley, J.; Nørskov, J. K.; Mavrikakis, M. *Annu. Rev. Phys. Chem.* **2002**, *53*, 319. (b) Hammer, B.; Nørskov, J. K. *Adv. Catal.* **2000**, *45*, 71.

(36) (a) Leskiw, B. D.; Castleman, A. W. *C. R. Physique* **2002**, *3*, 251. (b) Guo, B. C.; Kerns, K. P.; Castleman, A. W. *Science* **1992**, *225*, 1411. (c) Guo, B. C.; Wei, S.; Purnell, J.; Buzza, S.; Castleman, A. W. *Science* **1992**, *256*, 511.

(37) Rohmer, M. M.; Benard, M. *Chem. Rev.* **2000**, *100*, 495 and references therein.

(38) (a) Delley, B. *J. Chem. Phys.* **1990**, *92*, 508. (b) Delley, B. *J. Chem. Phys.* **2000**, *113*, 7756.

(39) Maiti, A.; Rodriguez, J. A.; Law, M.; Kung, P.; McKinney, J. R.; Yang, P. *Nano Lett.* **2003**, *3*, 1025.

(40) Hammer, B.; Hansen, L. B.; Nørskov, J. K. *Phys. Rev. B* **1999**, *59*, 7413.

(41) (a) Rodriguez, J. A.; Liu, P.; Dvorak, J.; Jirsak, T.; Gomes, J.; Takahashi, Y.; Nakamura, K. *Phys. Rev. B* **2004**, *69*, 115414. (b) Rodriguez, J. A.; Liu, P.; Dvorak, J.; Jirsak, T.; Gomes, J.; Takahashi, Y.; Nakamura, K. *J. Chem. Phys.* **2004**, *121*, 465.

(42) Lewis, K. E.; Golden, S. M.; Smith, G. P. *J. Am. Chem. Soc.* **1984**, *106*, 3095.

(43) (a) Mulliken, R. S. *J. Chem. Phys.* **1955**, *23*, 1833. (b) Chang, H.; Harrison, J. F.; Kaplan, T. A.; Mahanti, S. D. *Phys. Rev. B* **1994**, *49*, 15753. (c) Bauschlicher, C. W., Jr.; Bagus, P. S. *J. Chem. Phys.* **1984**, *81*, 5889.

(44) St. Clair, T. P.; Oyama, S. T.; Cox, D. F.; Otani, S.; Ishizawa, Y.; Lo, R. L.; Fukui, K.; Iwasawa, Y. *Surf. Sci.* **1999**, *426*, 187.

(45) Otani, S.; Ishizawa, Y. *J. Cryst. Growth* **1995**, *154*, 202.

(46) Hugosson, H. W.; Nordström, L.; Jansson, U.; Johansson, B.; Eriksson, O. *Phys. Rev. B* **1999**, *60*, 15123.

(47) (a) Pilgrim, J. S.; Duncan M. A. *J. Am. Soc.* **1993**, *115*, 6958. (b) Lightstone, J. M.; Mann, H. A.; Wu, M.; Johnson, P. M.; White, M. G. *J. Phys. Chem. B* **2003**, *107*, 10359.

(48) Clark, A. H.; Beagley, B. *Trans. Faraday Soc.* **1971**, *67*, 2216.

(49) (a) Kwiatkowski, J. S.; Leszczynski, J.; Teca, I. *J. Mol. Struct.* **1997**, *436−437*, 451. (b) Bak, B.; Christensen, D.; Hansen-Nygaard, L.; Rastrup-Anderson, J. *Mol. Spectrosc.* **1961**, *7*, 58.

(50) Kochikov, I. V.; Tarasov, Y. I.; Sporidonov, V. P.; Kuramshina, G. M.; Rankin, D. W. S.; Saakjan, A. S. *J. Mol. Struct.* **2001**, *567*, 29.

(51) Sakai, Y.; Koyanagi, M.; Mogi, K.; Miyoshi, E. *Surf. Sci.* **2002**, *513*, 272.

(52) Kupka, T.; Wrzalik, R.; Pasterna, G.; Pasterny, K. *J. Mol. Struct.* **2002**, *616*, 17.

(53) Majumder, C.; Briere, T. M.; Mizuseki, H.; Kawazoe, Y. *J. Chem. Phys.* **2002**, *117*, 2819.

(54) Liu, P.; Nørskov, J. K. *Phys. Chem. Chem. Phys.* **2001**, *3*, 3814.

(55) Rodriguez, J. A.; Jirsak, T.; Chaturvedi, S.; Kuhn, M. *Surf. Sci.* **1999**, *442*, 400.

(56) Jirsak, T.; Dvorak, J.; Rodriguez, J. A. *J. Phys. Chem. B* **1999**, *103*, 550.

(57) Quigley, W. W. C.; Yamamoto, H. D.; Aegerter, P. A.; Simpson, G. J.; Busell, M. E. *Langmuir* **1996**, *12*, 1500.

(58) Liu, G.; Rodriguez, J. A.; Hrbek, J.; Long, B. T.; Chen, D. A. *J. Mol. Catal. A: Chem.* **2003**, *202*, 215.

(59) Lopez, N.; Nørskov, J. K. *J. Am. Chem. Soc.* **2002**, *124*, 11262.

(60) Giordano, L.; Pacchioni, G.; Illas, F.; Rösch, N. *Surf. Sci.* **2002**, *499*, 73.

(61) González, S.; Sousa, C.; Fernandez-García, M.; Bertin, V.; Illas, F. *J. Phys. Chem. B* **2002**, *106*, 7839.

(62) (a) Molina, L. M.; Hammer, B. *Phys. Rev. Lett.* **2003**, *90*, 206102. (b) Häkkinen, H.; Abbet, S.; Sanchez, A.; Heiz, U.; Landman, U. *Angew. Chem., Int. Ed.* **2003**, *42*, 1297. (c) Rodriguez, J. A.; Pérez, M.; Jirsak, T.; Evans, J.; Hrbek, J.; González, L. *Chem. Phys. Lett.* **2003**, *378*, 526.